DESIGN AND SYNTHESIS OF METAL-ORGANIC FRAMEWORK AND ITS BIOMEDICAL APPLICATIONS

M.Sc. Thesis

By
SHREYA TYAGI

DEPARTMENT OF CHEMISTRY
INDIAN INSTITUTE OF TECHNOLOGY INDORE
MAY 2024

DESIGN AND SYNTHESIS OF METAL-ORGANIC FRAMEWORK AND ITS BIOMEDICAL APPLICATIONS

A THESIS

Submitted in partial fulfillment of the
requirements for the award of the degree
of
Master of Science

by
SHREYA TYAGI

DEPARTMENT OF CHEMISTRY
INDIAN INSTITUTE OF TECHNOLOGY INDORE
MAY 2024

INDIAN INSTITUTE OF TECHNOLOGY INDORE

CANDIDATE'S DECLARATION

I hereby certify that the work which is being presented in the thesis entitled **"Design and Synthesis of Metal-Organic Framework and its Biomedical Applications** in the partial fulfillment of the requirements for the award of the degree of **MASTER OF SCIENCE** and submitted in the **DEPARTMENT OF CHEMISTRY, Indian Institute of Technology Indore**, is an authentic record of my own work carried out during the time period from July 2023 to May 2024 under the supervision of Prof. Shaikh M. Mobin, Professor, Department of Chemistry, IIT Indore.

The matter presented in this thesis has not been submitted by me for the award of any other degree of this or any other institute.

Signature of the student with date
(SHREYA TYAGI)

This is to certify that the above statement made by the candidate is correct to the best of my/our knowledge.

May 17, 2024

Signature of thesis Supervisor with date
(Prof. Shaikh M. Mobin)

SHREYA TYAGI has successfully given her M.Sc. Oral Examination held on **… May**.

Signature of Supervisor of M.Sc. thesis
Date: May 17, 2024

Convener, DPGC
Date:

Signature of PSPC Member 1
Date:

Signature of PSPC Member 2
Date:

ACKNOWLEDGEMENTS

I extend heartfelt gratitude to my supervisor **Prof. Shaikh M. Mobin** for constantly guiding, supporting, and encouraging me in the duration of this project. His valuable inputs have helped me learn a lot of skills which shall prove to be very fruitful throughout my research experience. I am also thankful to the PSPC committee members **Prof. Dr. Sampak Samanta** and **Dr. Pravarthana Dhanapal** for their valuable guidance, insightful feedback and constructive criticism.

I also take the opportunity to thank our honourable Director **Prof. Suhas Joshi** and Head of the Department **Prof. Tushar Kanti Mukherjee**, IIT Indore for providing the infrastructure and necessary environment to carry out the research. I would like to thank the entire **Faculty members** of IIT Indore and **SIC** for constantly showing a supporting gesture.

I express my sincere thanks to my seniors **Mr. Rakesh Deka**, **Mr. Praveen Kumar**, **Mrs. Reena Kyarikwal**, **Ms. Nirmiti Mate**, **Ms. Vinita Satwani**, **Mr. Nitin Rajesh** for their generous help and constant support. I would also like to thank my **friends** for motivating me during the work of the project. I would like to thank **Mr. Kinney Pandey**, **Mr. Ghanshyam Bhavsar**, **Er. Atul Singh** and **Mr. Manish Kushwaha**, **Mr. P.K. Parthiban** for the technical support and assistance throughout the year.

Most importantly, it would have been impossible for me to reach here without the support, care, and love of my family members. I would like express my gratitude to my parents **Mr. Nirdosh Tyagi** and **Mrs. Anuradha Tyagi**, my brother **Mr. Saksham Tyagi**, my **grandparents**, my **uncle** and **aunty**, and my **cousins** for their constant motivation throughout my life and for always being understanding and supporting in every situation.

SHREYA TYAGI

Dedicated to

MY FAMILY

Abstract

Over the past decades, the usage of metal-organic frameworks (MOFs) in biomedical applications has increased significantly because these materials have high loading capacities, high surface areas, and precision tunability. Moreover, a wide range of drug delivery applications are being investigated for MOFs. Herein, we have synthesized copper-based MOFs (**IITI-3**) which were characterized by using PXRD, TGA, BET, IR, and UV techniques. In this study, we have analyzed the effective delivery of two drugs using IITI-3: Ibuprofen and Curcumin. Brunauer-Emmett-Teller (BET) analysis affirmed the IITI-3's suitability as a carrier, demonstrating its ability to accommodate multiple drugs simultaneously. Interestingly, while simultaneous loading of both drugs was successful, individual drug loading experiments revealed selective encapsulation of only Curcumin within IITI-3. The pH-dependent release of the encapsulated drugs was validated by further release investigations employing UV spectroscopy at pH 7.4 and 5.8, which represent physiological and second intestine pH respectively. This pH-responsive behavior has potential use in targeted drug administration, especially in conditions similar to second intestine pH

TABLE OF CONTENTS

LIST OF SCHEMES

LIST OF FIGURES

NOMENCLATURE

λ	Wavelength
Å	Angstrom
nm	Nanometer
cm	Centimeter
º	Degree
K	Kelvin
M	Molar
mM	Millimolar
µM	Micromolar
mL	Milliliter
mg	Milligram
g	Gram
µL	Microliter
a.u.	Arbitrary unit
pH	Potential of Hydrogen

ACRONYMS

NMOFs	Nanoscale Metal-Organic Frameworks
MOFs	Metal-Organic Frameworks
DDS	Drug Delivery System
PCPs	Porous Co-ordination Polymers
VOCs	Volatile Organic Compounds
MRI	Magnetic Resonance Imaging
CT	Computed tomography
AD	Alzheimer's Disease
UV-vis	Ultraviolet-visible
NMR	Nuclear magnetic Resonance
FE-SEM	Field emission scanning electron microscopy
SEM	Scanning electron microscope
PXRD	Powder X-ray diffraction
TGA	Thermogravimetric Analysis
IR	Infrared
BET	Brunauer-Emmett-Teller
RPM	Rotations per minute
DI	Deionized
SM	Starting Material
LEA	Ester
LHA	Acid
IITI-3-D	Dual drug loaded MOF

Chapter 1

Introduction

Enhancing human health and elongating lifespan require the advancement of therapeutic solutions, encompassing chemical agents and bioactive compounds. Many of these compounds exhibit potential in addressing acute ailments like cancer, diabetes, cardiovascular issues[1-5], renal disorders, and microbial infections[1]. However, their widespread application in medicine faces substantial impediments, including poor solubility, inefficient absorption, limited bioavailability, and indiscriminate distribution in the body, often resulting in adverse effects on healthy tissues[2-4].

To surmount these challenges, the adoption of nano-based drug delivery systems (DDS) emerges as a promising strategy[6]. Nanostructures offer avenues for enhancing drug solubility and stability, controlled release of drug, increased bioavailability, minimized toxicity, and targeted delivery to specific anatomical sites. Consequently, interdisciplinary efforts spanning chemistry, biochemistry, medicine, and biomedical engineering persistently strive to innovate efficient DDS solutions[6-9].

Nanotechnology revolutionizes various domains, including biomedical, biological, environmental, and nutraceutical research[9-11], through the deployment of nanostructures like nanofibers, nanoparticles, nanotubes, and nanocomposites. These structures not only aid in disease diagnosis[12] and treatment[10,13,14] but also serve as carriers for drugs[15], proteins[16], vaccines[17], genes[18], and enzymes[19], heralding the dawn of nanomedicine[15,16]. This burgeoning field harnesses nanoscience to combat diseases, utilizing nanodimensional entities such as nanovehicles, nanosensors, and nanorobots for diagnostic and therapeutic purposes within living organisms[15-20].

Nanocarriers[3,28], colloidal systems comprising submicron particles or droplets, exhibit superior mobility within the human body owing to their diminutive size. Their distinctive chemical, structural, magnetic, and biological properties render them invaluable in drug delivery applications[20-27]. These carriers, whether organic, inorganic, or hybrid, encapsulate or conjugate therapeutic agents[28,29,30], facilitating their targeted delivery, prolonged circulation, and controlled release kinetics[30-38].

Moreover, advancements in nanotechnology have engendered diverse strategies for drug delivery[39-41], including passive and self-delivery mechanisms. Passive delivery involves chemical conjugation or physical encapsulation of drugs with nanostructures, while self-delivery relies on

drugs' inherent ability to self-assemble within nanostructures[42,43]. Each approach offers unique advantages in terms of controlled release and targeting precision, albeit with distinct mechanisms of action[38].

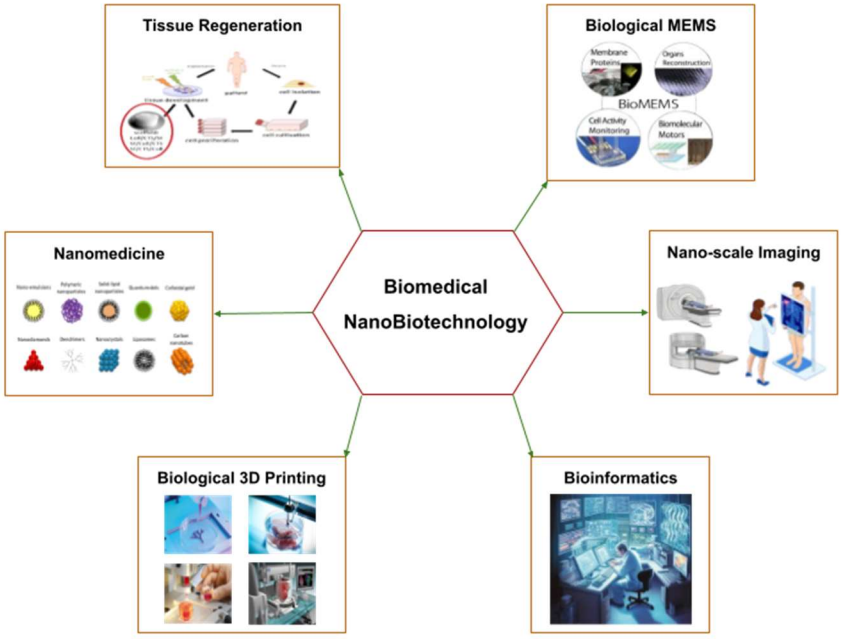

Figure 1: Nanotechnology applications in the biomedical field[39][40][41].

In the realm of nanocarrier selection, the biomedical community grapples with the challenge of identifying the most suitable type for specific applications. Metal-organic framework (MOF) nanocarriers have garnered attention for their multifaceted utility in delivering biomolecules, yet comprehensive investigations into their potential as drug delivery vehicles and biosensors remain scarce. Thus, the recent advancements in MOFs as a favourable nanocarriers for diagnosis of various diseases and drug delivery needed to be elucidate. By delineating their synthesis, applications, and therapeutic potentials across various diseases, including cancer, diabetes (type I, II), and Alzheimer's disease.

1.1. Metal-Organic Framework (MOFs)

Metal-organic frameworks, affectionately referred as porous coordination polymers (PCPs)[44,45], represent a class of porous crystalline materials characterized by their tunable nature.

These structures arise from the self-assembly of organic ligands and inorganic metal clusters, resulting in extended network structures[46]. The dynamic combination of organic linkers and metal ions yields diverse MOF structures with highly porous frameworks, distinguishing them from other nanostructures[47-52].

MOFs have garnered significant interest due to their exceptional properties, driving research across various fields. These applications span gas storage and separation, bioimaging, water treatment, catalysis, chemical separation, and energy-related endeavours[52-59]. Notably, MOFs exhibit high surface area and porosity, enabling efficient loading of biomolecules and pharmaceuticals, alongside adjustable pore sizes conducive to selective molecular encapsulation. Their open architectures facilitate interactions with external environments, while their diverse compositions allow tailored designs to suit specific applications[59-61].

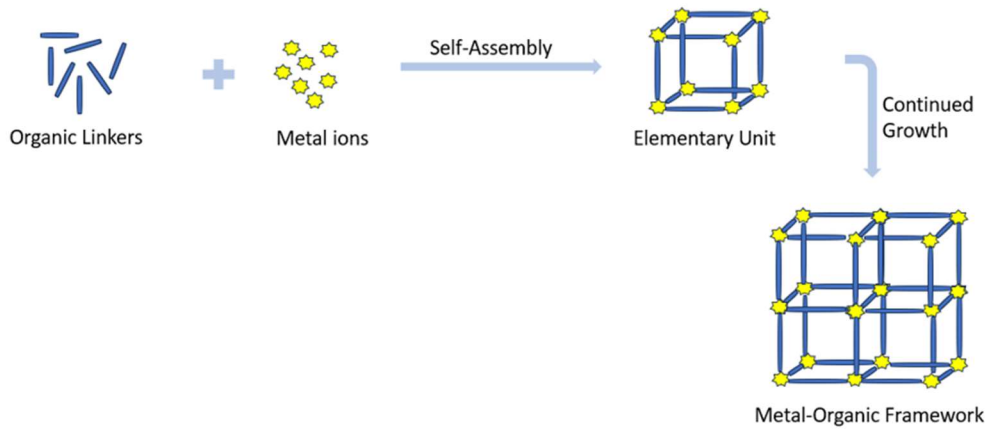

Figure 2: Metal-Organic Frameworks

Moreover, MOFs possess attributes such as biodegradability[47,62], owing to weak coordination bonds, and high crystallinity, providing insights into their morphological characteristics and network structures[60-63]. These properties position MOFs as promising candidates for biomedical applications, particularly diagnosis of disease and the drug delivery[64].

In biomedical contexts, mastering control over the size and morphology of MOF is crucial, as particles smaller than 100 nm can only effectively penetrate cells[64-66]. The emergence of nanoscale MOFs (NMOFs) bring forward enhanced functionalities, merging the structural diversity of bulk MOFs with benefits of nanomaterials[65]. The chemical and catalytic activities of NMOFs are influenced by factors such as size, shape, and surface characteristics. Synthesizing NMOFs

presents a burgeoning area of research, encompassing methods such as surface-assisted synthesis, sonochemical and microwave-assisted synthesis, coordination modulation and microemulsion synthesis. These endeavours aim to exploit the unique properties of NMOFs for diverse biomedical applications[65-72].

1.2 Synthesis of MOFs

The synthesis of Metal-Organic Frameworks (MOFs) encompasses a myriad of experimental conditions that intricately influence their resulting crystallinity[67], porosity and morphology. Selecting an appropriate synthesis method becomes pivotal in tailoring the physicochemical properties of the acquired products to meet specific application requirements[71-74]. Moreover, considerations must extend beyond mere scientific parameters to encompass economic feasibility and environmental sustainability, particularly concerning large-scale synthesis endeavours. Various synthetic techniques are available for the generation of MOFs, each offering its own set of advantages and challenges[75,78].

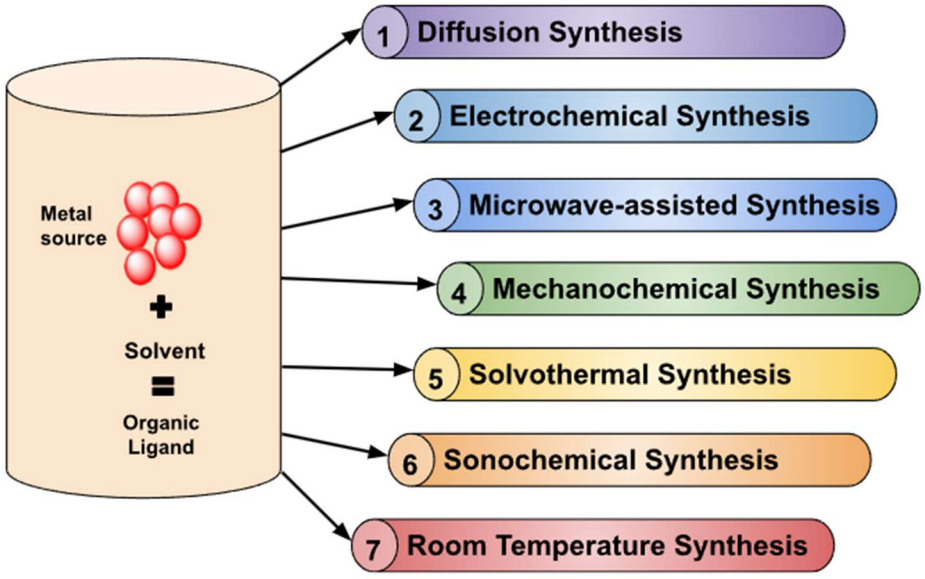

Figure 3: MOF synthesis methods.

1.3. Solvothermal Method

The solvothermal method, a cornerstone of MOF synthesis, continues to be widely adopted owing to its versatility and reproducibility. The method involves the reaction between organic ligands and metal salts in a solvent-based environment, conducted under elevated pressure and temperature within a sealed vessel. The selection of solvent significantly influences reaction kinetics and reagent solubility, with traditional electric heating serving as the primary energy source[67]. Noteworthy applications include the synthesis of diverse MOFs using organic solvents such as acetone, ethanol, and dimethylformamide, highlighting the versatility and scalability of this method[79,91].

In conclusion, the synthesis of MOFs encompasses a diverse array of techniques, each offering unique advantages and challenges. From diffusion-based methods to advanced microwave-assisted synthesis, the field of MOF synthesis continues to evolve, driven by a relentless pursuit of sustainability, efficiency, and versatility. As researchers continue to explore novel synthesis routes and optimize existing methodologies, the future of MOF synthesis holds boundless potential for addressing pressing societal and environmental challenges.

1.4. Bio-medical Applications of MOFs

MOFs have emerged as versatile platforms with profound implications in various biomedical applications owing to their remarkable properties. These include biodegradability, biocompatibility, high porosity, large pore size, nanometer-scale dimensions and extensive surface area[92-94]. Leveraging these attributes, MOFs have showcased immense potential in bioimaging, drug delivery, biocatalysis and biosensing, each delineating a unique pathway towards advancing healthcare paradigms[94,96].

In the realm of drug delivery, MOFs serve as proficient carriers capable of entrapping biomolecules within their cavernous structures or adsorbing them during synthesis. Their expansive surface area, spanning from 1000 to 10,000 m2/g[96,98], coupled with tunable pore sizes spanning from microporous to mesoporous, enables efficient encapsulation of diverse functional molecules. Notably, achieving a particle size below 200 nm facilitates unhindered circulation within the intricate network of capillaries, ensuring targeted delivery to specific anatomical sites[98-102]. One

notable approach involves de novo synthesis, where MOF substrate encapsulation and formation occur concomitantly, facilitating the immobilization of molecules surpassing the pore dimensions.

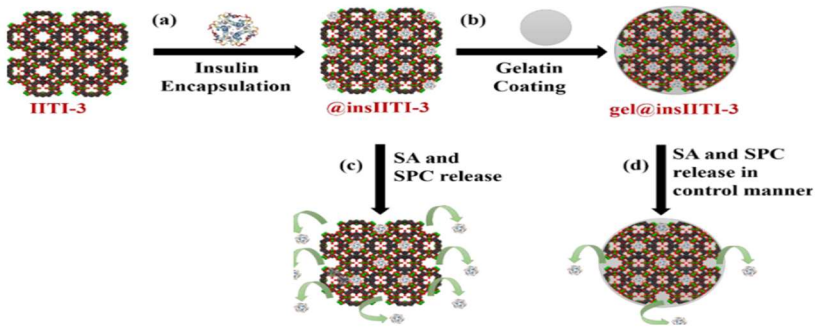

Figure 4: (a) Insulin encapsulation IITI-3 and the (b) gelatin coating on insIITI-3; panels (c) and (d) show insulin release profiles from insIITI-3 and gel@insIITI-3 in stomach acid and SPC pH, respectively[137]. (Permission Granted).

Beyond drug delivery, MOFs have garnered considerable attention in biosensing applications, capitalizing on their expansive specific surface areas and diverse pore geometries. Through various conjugation techniques, MOFs facilitate the design of biosensors capable of detecting small molecules, proteins, ions, cancer cells and nucleic acids with high specificity and sensitivity. Additionally, MOFs serve as promising nanozymes, mimicking the catalytic environments of natural enzymes and finding utility in enzymatic reactions critical for biosensing applications[101].

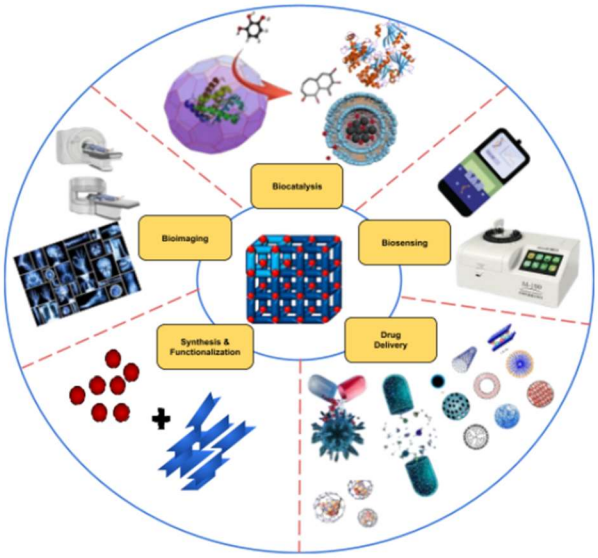

Figure 5: Biomedical Application of MOF[103][104][105].

In the domain of bioimaging, MOFs offer a multifaceted approach towards developing targeted platforms for various imaging modalities, including optical molecular imaging, magnetic resonance imaging (MRI) and X-ray computed tomography (CT) imaging[47]. By modulating imaging contrast agents, MOFs enable precise visualization of biological structures and processes, thereby enhancing diagnostic accuracy and therapeutic efficacy.

In summary, the burgeoning field of MOF-based biomedical applications heralds a new era of innovation in healthcare delivery and disease management. With ongoing advancements in synthesis methodologies and material design, MOFs are poised to revolutionize drug delivery, biosensing, bioimaging, and biocatalysis[106].

Chapter 2

Past Work

MOFs have garnered considerable attention as a promising platform for controlled drug delivery, disease diagnosis, and theranostic applications, which combine both diagnostic and therapeutic functionalities. This section delves into the diverse applications of MOFs across various diseases that pose significant threats to global health.

2.1 Treatment of Cancer

Cancer remains a paramount public health concern worldwide, accounting for millions of deaths annually[106]. It manifests as a genetic anomaly characterized by aberrant cell proliferation and metastasis, posing a substantial burden on healthcare systems globally. Consequently, extensive efforts across multidisciplinary research domains have been directed towards devising innovative and efficacious strategies for cancer treatment and diagnosis. In the realm of cancer diagnosis, MOFs have emerged as promising candidates. For instance, Kong et al.[107] explored the potential of a green-emission Zr(IV)-MOF (BUT-88) as a biosensing platform for breast cancer cells (MCF-7 cells), achieving enhanced detection precision for dual tumor biomarkers, MUC-1 and miRNA-21. Their study exemplified the capability of MOF-based fluorescent nanoprobe technology to identify specific cancer biomarkers, facilitating early cancer detection with high sensitivity and specificity.

2.2. Treatment of Diabetes

Diabetes, a multifaceted metabolic disorder, poses a formidable challenge to global public health. This chronic condition, characterized by inadequate insulin production or ineffective utilization of insulin[108-114], results in dysregulated blood glucose levels. The ramifications of diabetes extend far beyond glycemic control, encompassing a spectrum of complications that affect virtually every organ system in the body[111]. From microvascular complications like nephropathy and retinopathy to macrovascular complications like cardiovascular disease, diabetes exacts a heavy toll on individuals and healthcare systems worldwide. Recent research endeavours have explored innovative approaches to diabetes diagnosis, with a particular focus on non-invasive methods like breath analysis. Exhaled breath contains volatile organic compounds (VOCs), including acetone, which serve as potential biomarkers for diabetes[111,114]. MOFs have emerged as promising candidates for developing sensitive and selective sensors capable of detecting acetone in breath samples[115]. Effective management of diabetes hinges on precise monitoring of blood glucose levels, a task facilitated by advanced sensor technologies[118]. Electrochemical enzyme-free sensors, empowered by MOFs, have emerged as front-runners in the quest for accurate and reliable glucose detection. In the realm of diabetes therapeutics, the quest for innovative drug delivery systems has led researchers to explore the untapped potential of MOFs. Recognizing the need for alternative insulin delivery methods, Chen et al.[119] embarked on a quest to harness the encapsulation capabilities of MOFs for oral insulin delivery. By ingeniously leveraging the unique physicochemical properties of MOFs, they engineered crystalline zirconium-based mesoporous frameworks capable of protecting insulin from gastric degradation while facilitating controlled release in the bloodstream[120-128,137].

2.3. Treatment of Alzheimer's Disease

Alzheimer's disease (AD), the most common type of dementia globally, poses a significant public health challenge with profound socioeconomic implications[126]. Characterized by progressive cognitive decline, memory loss, and functional impairment, AD exacts a heavy toll on individuals and healthcare systems alike, particularly as life expectancy continues to rise. Mounting evidence suggests that dysregulation of metal ions such as Cu^{2+}, Fe^{3+}, Al^{3+}, and Zn^{2+} may contribute to the pathogenesis of AD, underscoring the urgent need for innovative diagnostic and therapeutic

strategies [130-133]. MOF-based fluorescent biosensors have emerged as powerful tools for detecting aberrant metal ion levels implicated in AD pathophysiology [133,134]. These biosensors leverage the unique optical properties of MOFs to selectively bind and detect metal ions with high sensitivity and specificity, offering unprecedented insights into the molecular mechanisms underlying AD progression [135].

2.4. Treatment of Ocular Diseases

Ocular diseases represent a leading cause of vision impairment worldwide, posing significant challenges for both patients and clinicians. From glaucoma to macular degeneration, these conditions encompass a broad spectrum of disorders that can profoundly impact visual acuity and quality of life[136]. However, traditional ocular drug delivery methods are fraught with challenges, with only a fraction of administered drugs reaching their intended target tissues.

MOFs have emerged as promising nanocarriers for drug delivery curing ocular diseases, offering enhanced biocompatibility, sustained release kinetics, and targeted delivery to intraocular tissues. By encapsulating therapeutic agents within the porous framework of MOFs, researchers have unlocked new possibilities for overcoming the limitations of conventional drug delivery systems and improving treatment outcomes for ocular diseases[136].

Overall, MOF-based sensing technologies hold great promise for the rapid and accurate detection of various diseases and infections, while MOF-based drug delivery systems offer innovative approaches to the treatment of these diseases and bacterial infections[136]. Continued research in this field is essential for the development of novel therapeutics and diagnostics to address the ongoing challenges posed by infectious and non-infectious diseases.

Chapter 3

Experimental Section

3.1. Materials

All reagents were commercially available and were used without any further purification. 5-hydroxyphthalic acid (98.00%) was bought from Alfa Aesar. $Cu(NO_3)_2.3H_2O$ (98.00%) and Curcumin (95.00%) were bought from Sisco Research Laboratories. Sodium hydroxide (NaOH) pellets were bought from Rankem. Potassium carbonate (K_2CO_3) (98.00%) was bought from Emplura. Ibuprofen (2-(4-Isobutylphenyl)propanoic acid) (99.92%) was bought from BLD Pharma. 2,6-Bis(bromomethyl)pyridine (>99.00%) was bought from TCI. Potassium hydroxide (KOH) pellets (85.00%) were bought from Aura. Ethanol (EtOH) (99.90%) was bought from CSS.

3.2 Synthesis of MOF

3.2.1 Synthesis of Diethyl 5-hydroxyphthalate

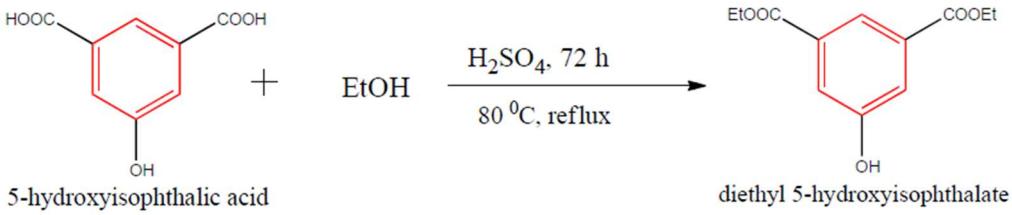

Scheme 1.1

In a round bottom flask a solution of 5-hydroxyisophthalic acid (5 g) and conc. H_2SO_4 (1.5 ml) was taken in anhydrous ethanol (35 ml) and stirred for 72 hours under refluxing. This solution was then allowed to cool at room temperature. After removal of the solvent under vacuum, the crude white product was dissolved in ice cold water and neutralized by sodium

carbonate. Acetonitrile was added to the product and heated to 80 ˚C for 5 more minutes. Product yield was found to be 4 g (80%) (**scheme 1.1**)[140].

3.2.2 Synthesis of tetraethyl 5,5'-((pyridine-2,6 diylbis(methylene))bis(oxy))diisophthalate

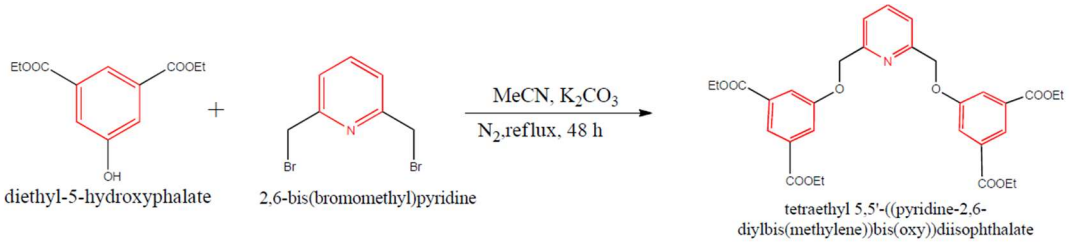

Scheme 1.2

In a 250 ml round bottom flask 5-hydroxyisophthalic acid diethyl ester (0.377 g) and potassium carbonate (0.417 g) were taken in dry acetonitrile(40ml) and stirred for 30 minutes at 60 ˚C. This reaction was then treated with 2,6-bis(bromomethyl)pyridine (0.20 g) and the temperature was raised to 85 ˚C under inert atmosphere of nitrogen and was allowed to reflux for 24 hours. Whole mixture was then allowed to cool at room temperature and poured into ice cold water to obtain white solid which was then collected in filter paper and dried in open air. Product yield was found to be 0.41 g (68%) (**scheme 1.2**)[140].

3.2.3 Synthesis of Linker (H_4L)

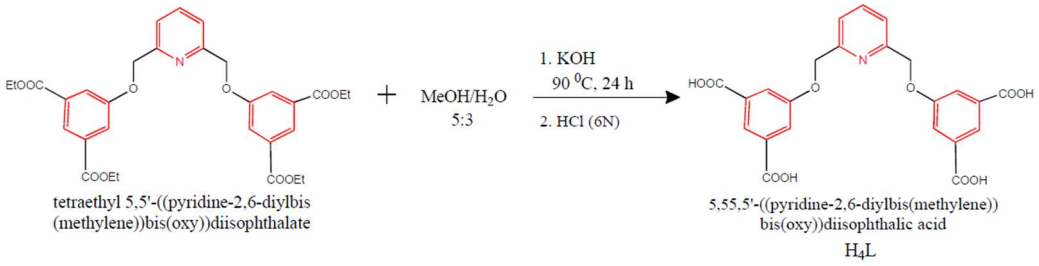

Scheme 1.3

The compound obtained as above (0.40 g) was hydrolysed by refluxing it with 6 N KOH solution (20 ml) for 24 hours. After cooling to 5 °C, the resulting solution was neutralized with 6

N HCl solution to obtain a white precipitate. It was collected and washed thoroughly with water and water dried. Product yield was found to be 320 mg (80%) (**scheme 1.3**)[140].

3.2.4 Synthesis of IITI-3

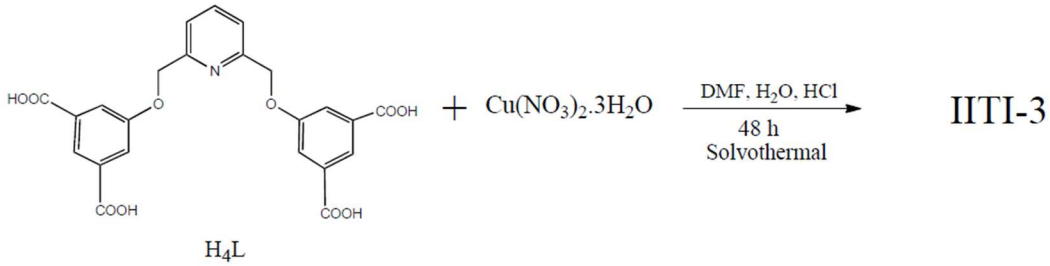

Scheme 1.4

IITI-3 was synthesized by using a mixture of H_4L (0.040 g), and $Cu(NO_3)_2 \cdot 3H_2O$ (0.120 g) in a mixture of DMF (4 ml) and water(2 ml) and 0.2 ml of 1 M HCl solution. This solution was mixed in 25 ml round bottom flask and was stirred for 1 hour and the resulting solution was packed and heated under high pressure in a Teflon-lined autoclave to 90 °C for 48 hours and with subsequent cooling to room temperature at the rate of 1 °C/min. The blue crystals of **IITI-3** were obtained. These crystals were continuously washed with water and acetone and air dried (yield = 77%) (**scheme 1.4**)[140].

3.3 Drug Loading Experiments

3.3.1 Activation of IITI-3

IITI-3 was activated prior to the drug loading experiment to obtain more porous and solvent-free material. Solvent exchange experiment using acetone was performed daily two times a day for 5 days. Further, the solvent exchanged sample was heated at 130 °C under extremely high vacuum conditions for 9 hours. A change in colour of the MOF was seen from green to dark blue due to the production of more pores and solvent free MOF. Activated MOF IITI-3 has high pore diameter because of the metal bounded water molecules' loss. **(Figure 6)**.

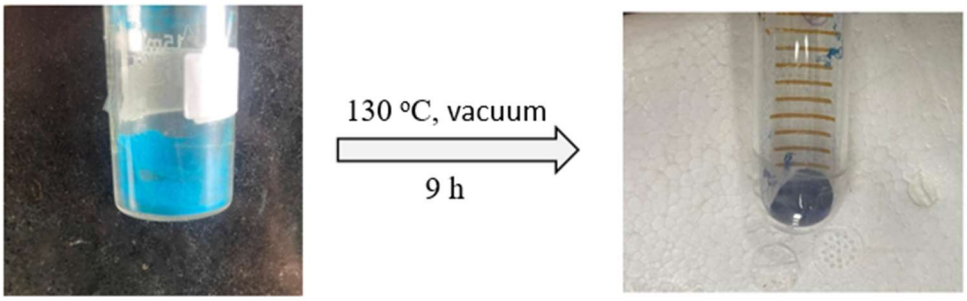

Figure 6: Activation of MOF

3.3.2 Dual Drug Loading

In a round bottom flask desired amount of drug that is 0.025 g of ibuprofen and 0.005 g of curcumin was taken in 20 ml of Methanol (30 wt% of IITI-3) and stirred for 30 minutes at room temperature. To this solution 0.1 g of IITI-3 was added and stirred at 450 rpm at room temperature for 24 hours. Solvent was evaporated after the completion of reaction and the sample of dual drug loaded **IITI-3-D** was washed 3 to 4 times with methanol. **IITI-3-D** (**Figure 7**) was analysed in IR, SEM and BET.

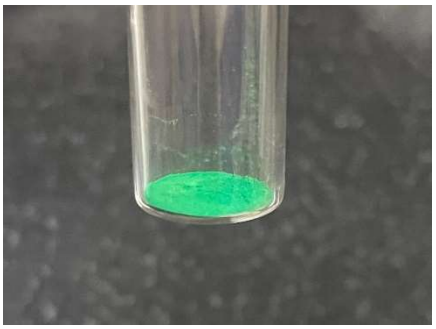

Figure 7: Dual drug (Ibuprofen and Curcumin) loaded MOF **IITI-3-D**

3.3.3 Ibuprofen Loading (24 hours)

In a test tube 0.01 g of IITI-3 was activated for 9 hours to which 3 ml of Ibuprofen solution (0.05 mg/ml) was poured and stirred at room temperature on 400 rpm. Samples have been taken after every 1 hour for 6 hours and then after 12 hours followed by the sample after 24 hours and were analysed using UV-Vis spectrometry. Linearity plots were plotted for the same.

3.3.4 Curcumin Loading (24 hours)

In a test tube 0.01 g of IITI-3 was activated for 9 hours to which 3 ml of Curcumin solution (0.01 mg/ml) was poured and stirred at room temperature on 400 rpm. Samples have been taken after every 1 hour for 6 hours and then after 12 hours followed by the sample after 24 hours and were analysed using UV-Vis spectrometry. Linearity plots were plotted for the same.

3.3.5 Ibuprofen Loading (72 hours)

In a test tube 0.01 g of IITI-3 was activated for 9 hours to which 3 ml of Ibuprofen solution (0.05 mg/ml) was poured and stirred at room temperature on 400 rpm. Samples have been taken after every 24 hours for 3 days and then were analysed using UV-Vis spectrometry. Linearity plots were plotted for the same.

3.3.6 Curcumin Loading (72 hours)

In a test tube 0.01 g of IITI-3 was activated for 9 hours to which 3 ml of Curcumin solution (0.01 mg/ml) was poured and stirred at room temperature on 400 rpm. Samples have been taken after every 24 hours for 3 days and then were analysed using UV-Vis spectrometry. Linearity plots were plotted for the same.

3.4 Drug Release Experiments

3.4.1 Drug Release at 5.8 pH

In a glass vial 10 mg drug loaded MOF was taken followed by the addition of 10 ml of a 5.8 pH DI water solution. The solution was stirred at 200 rpm for 36 hours. 2 ml sample was taken at every 1 hour for 6 hours and then after 12 hours, 24 hours and 36 hours and simultaneously 2 ml of 5.8 pH DI water solution was poured to the existing solution.

3.4.2 Drug Release at 7.4 pH

In a glass vial 10 mg drug loaded MOF was taken followed by the addition of 10 ml of a 7.4 pH DI water solution. The solution was stirred at 200 rpm for 36 hours. 2 ml sample was taken at every 1 hour for 6 hours and then after 12 hours, 24 hours and 36 hours and simultaneously 2 ml of 7.4 pH DI water solution was poured to the existing solution.

Chapter 4

Results and Discussion

4.1 Characterization of Linker

4.1.1 Mass Spectra of SM, LEA and LHA

ESI-MS spectra characterized the synthesized compounds SM, LEA and LHA. **SM** shows a base peak at m/z = 239.0893 (in positive mode) (**Figure 8**), **LEA** shows a base peak at m/z = 580.1878 (in positive mode) (**Figure 9**), and **LHA** shows a base peak at m/z = 466.0705 (in negative mode) (**Figure 10**).

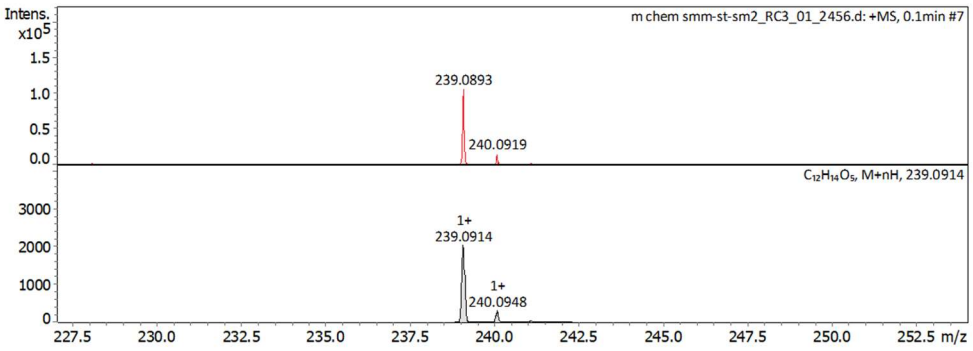

Figure 8: Mass spectrum of **SM**, ESI-MS (m/z) $C_{12}H_{14}O_5$: Calculated for $[C_{12}H_{14}O_5+H]$: 239.0948; Found: 239.0893

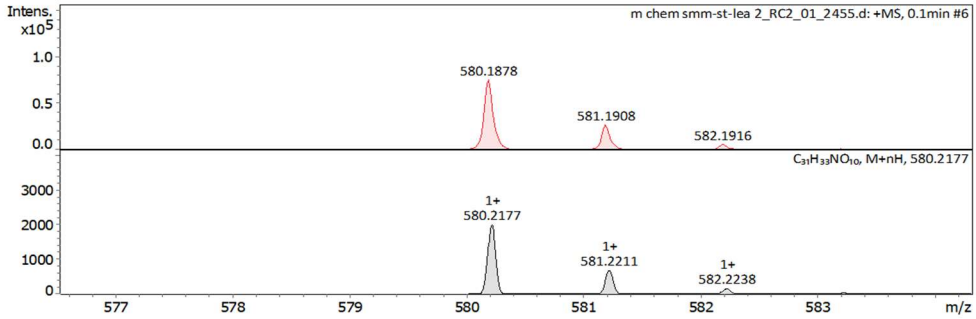

Figure 9: Mass spectrum of **LEA**, ESI-MS (m/z) $C_{31}H_{33}NO_{10}$: Calculated for $[C_{31}H_{33}NO_{10}+H]$: 580.2177; Found: 580.1878

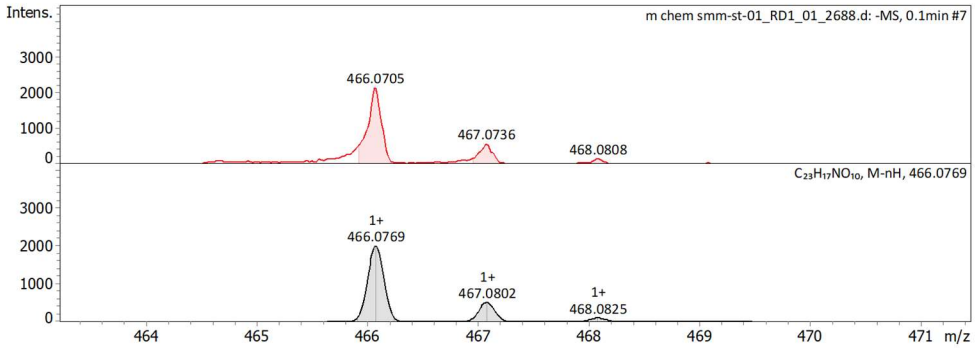

Figure 10: Mass spectrum of **LHA**, ESI-MS (m/z) $C_{23}H_{13}NO_{10}$: Calculated for $[C_{23}H_{13}NO_{10}-H]$: 466.0769; Found: 466.0705

4.1.2 NMR Spectra of LEA and LHA

NMR data for SM, LEA, and LHA molecules matched well with their proposed structures. ^{1}H NMR peaks in the δ 8.83-6.45 region correspond to the aromatic protons and a peak near 5.3ppm corresponds to the proton on secondary carbon next to O-atom. ^{13}C NMR peaks in the δ 120-160 region corresponds to aromatic carbons, peak above 160 ppm corresponds to the carbonyl carbon and peaks below 77.16 ppm corresponds to secondary, primary and carbon next to O-atom.

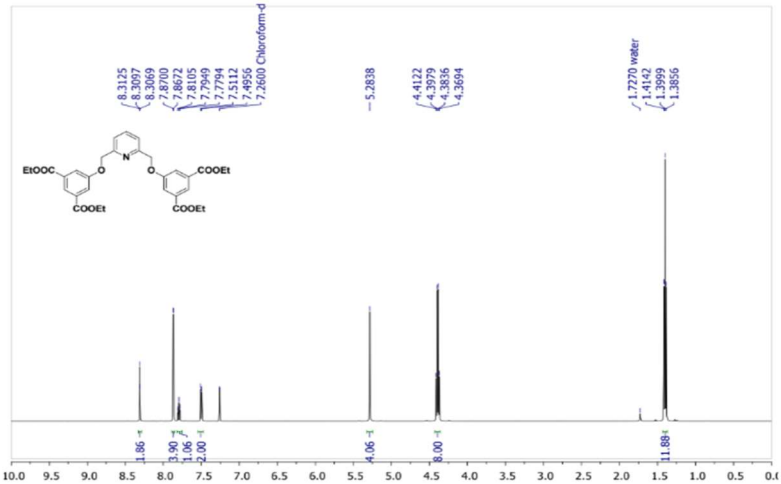

Figure 11: ^{1}H NMR of **LEA**. ^{1}H NMR (500 MHz, 298 K, $CDCl_3$) δ 8.31 (t, J = 1.4 Hz, 2H), 7.87 (d, J = 1.4 Hz, 4H), 7.79 (t, J = 7.8 Hz, 1H), 7.50 (d, J = 7.8Hz, 2H), 5.28 (s, 4H), 4.39 (q, J = 7.1 Hz, 8H), 1.40 (t, J = 7.1 Hz, 12H) ppm.

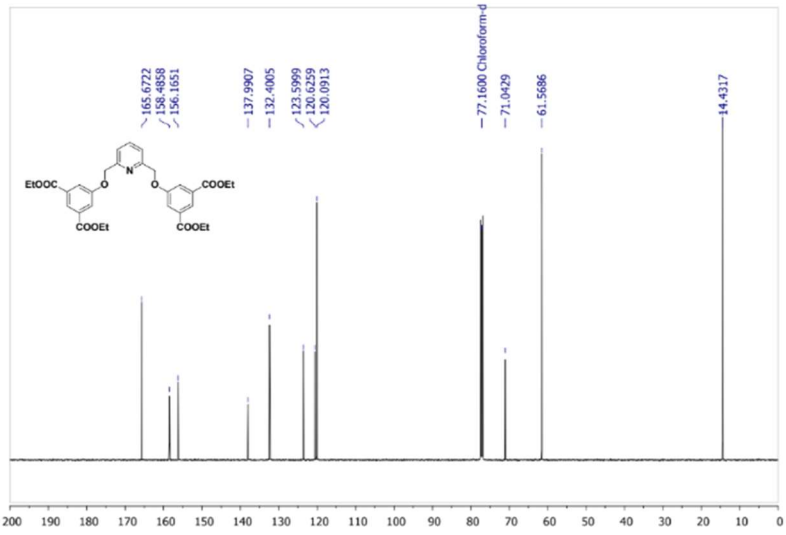

Figure 12: ^{13}C NMR of **LEA**. ^{13}C NMR (125 MHz, $CDCl_3$) δ 165.6, 158.4, 156.1, 137.9, 132.4, 123.6, 120.6, 120.1, 71.0, 61.57, 14.4 ppm

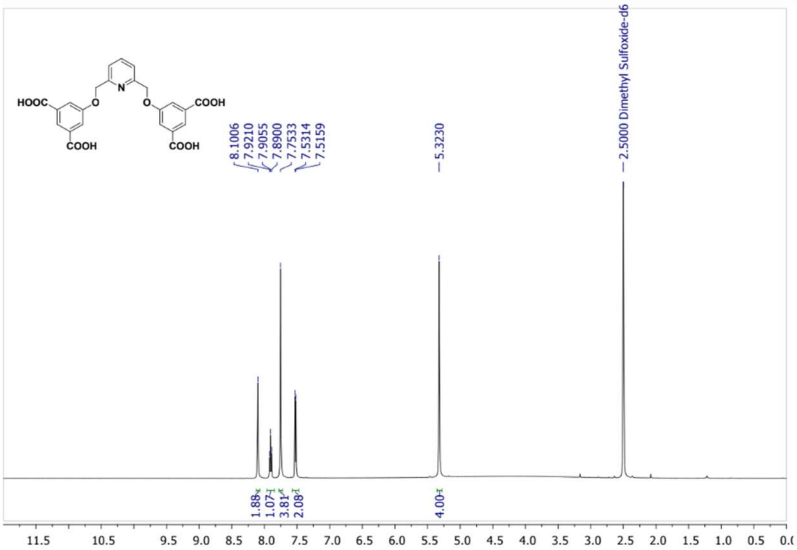

Figure 13: ^{1}H NMR of **LHA**. ^{1}H NMR (500 MHz, 298 K, DMSO-d6) δ 8.10 (s, 2H), 7.91 (t, J = 7.8 Hz, 1H), 7.75 (s, 4H), 7.52 (d, J = 7.7 Hz, 2H), 5.32 (s, 4H) ppm.

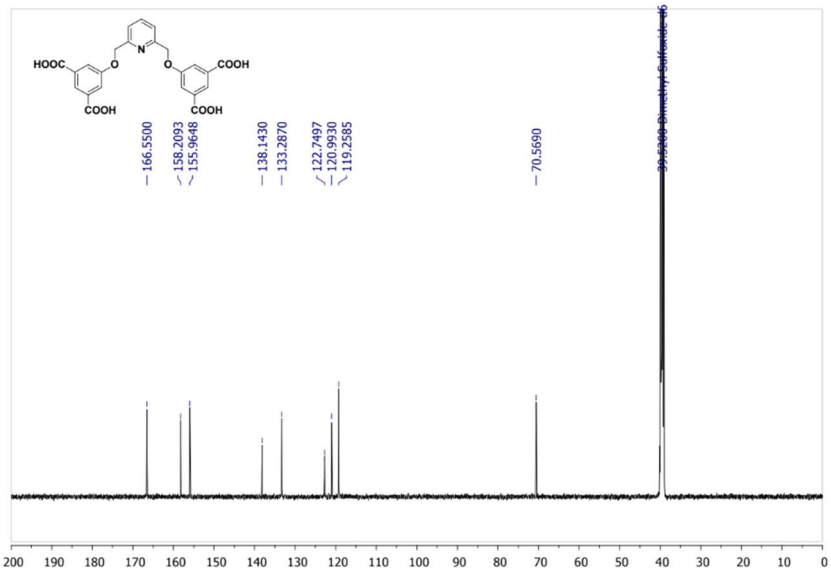

Figure 14: ^{13}C NMR of **LHA**. ^{13}C NMR (125 MHz, DMSO-d6) δ 166.5, 158.2, 155.9, 138.1, 133.2, 122.7, 120.9, 11.

4.2 Characterization of IITI-3

To calculate the surface area and pore size distribution of **IITI-3**, the N_2 sorption study is performed at 77 K. The BET surface area came out to be 730.902 m^2/g and pore diameter as 3.413 nm which confirms MOF to be both mesoporous and microporous. PXRD data confirms MOF to be crystalline in nature.

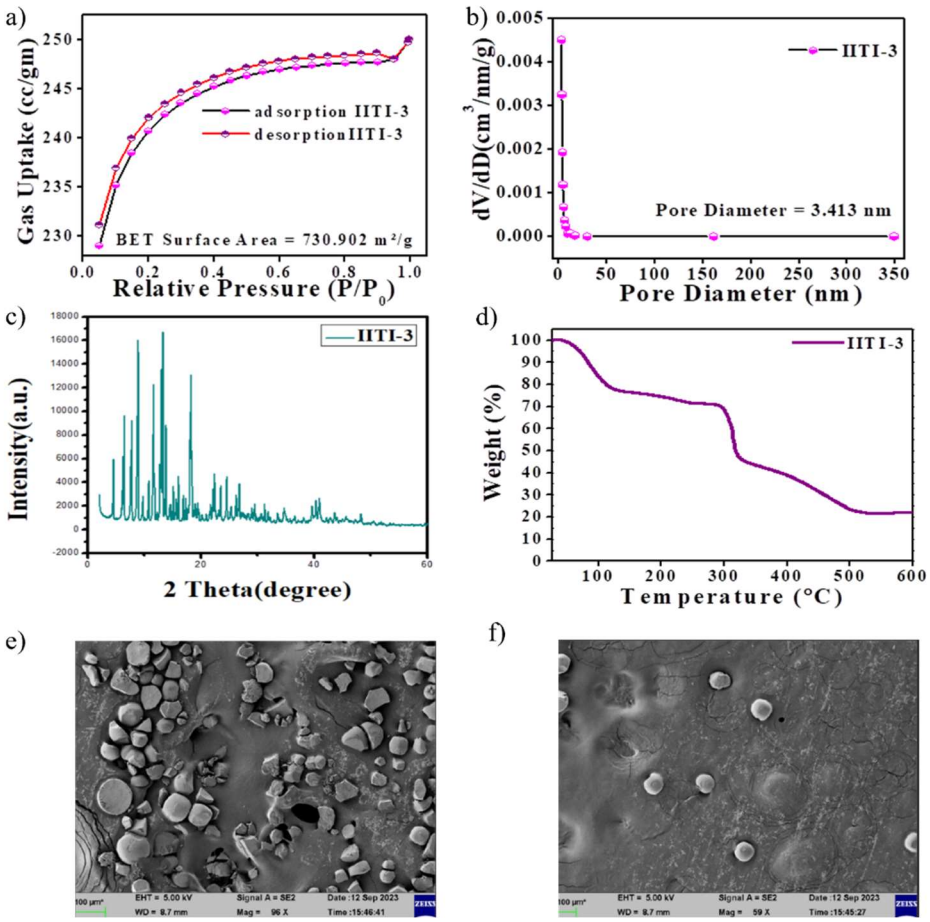

Figure 15: a) **BET** surface area analysis of **IITI-3,** b) **BJH** pore size distribution of **IITI-3**, c) **PXRD** data of **IITI-3**, d) Thermogravimetric analysis of **IITI-3**, e), f) **SEM** images of **IITI-3.**

4.3 Drug Loading Experiments

4.3.1 Data of Dual-drug Loading

To calculate the surface area and pore size distribution of **IITI-3-D**, the N_2 sorption study is performed at 77 K. The BET surface area decreased from an area of 730.902 m^2/g to 15.428 m^2/g and pore diameter from 3.413 nm to 3.392 nm confirms drugs are present on the surface as well as inside the pores. IR conforms the formation of new bonds and interactions.

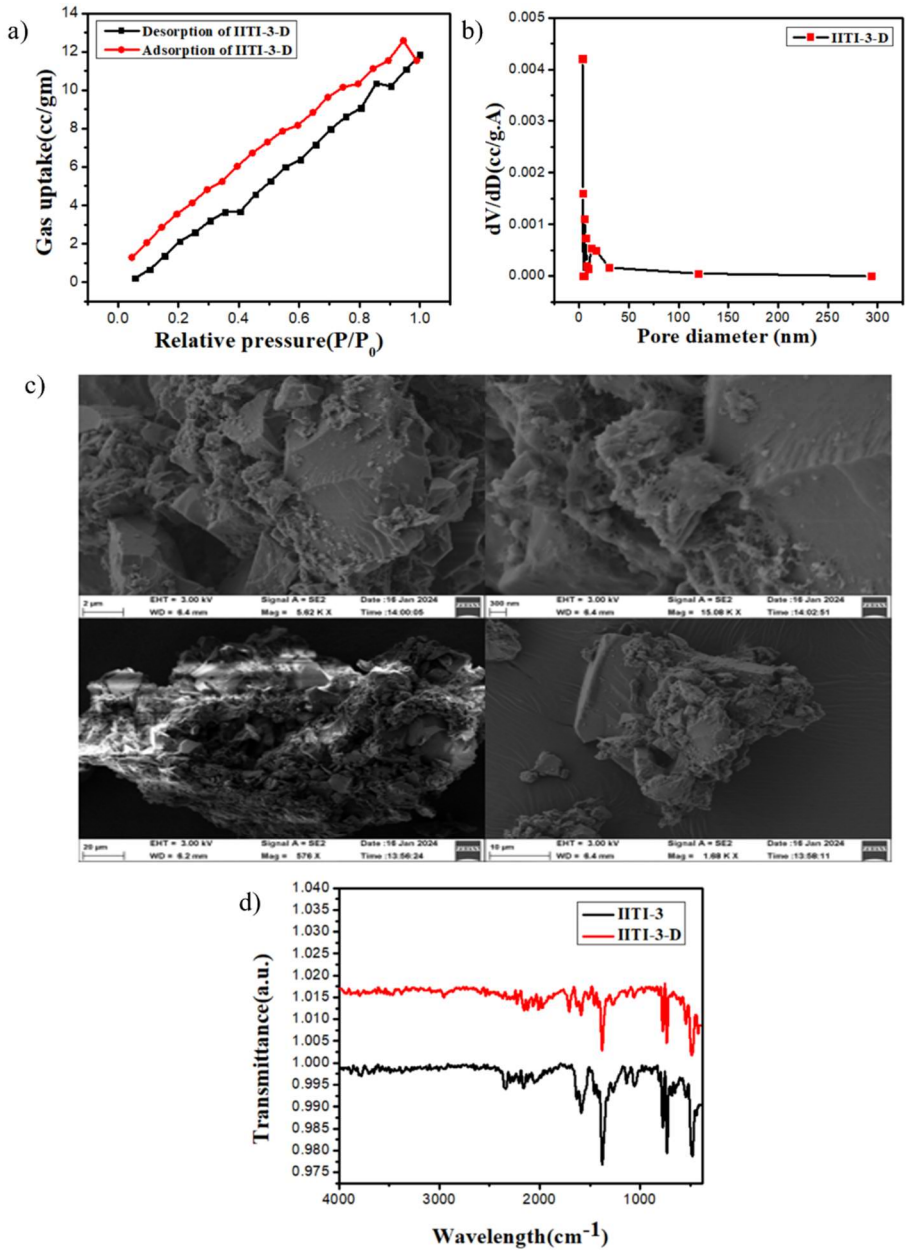

Figure 16: a) **BET** surface area analysis of **IITI-3-D**, b) **BJH** pore size distribution of **IITI-3-D**, c) **SEM** images of **IITI-3-D**, d) **IR** spectra of **IITI-3** and **IITI-3-D.**

4.3.2 Data of Ibuprofen Loading

UV-Vis data confirms that the loading have not occurred.

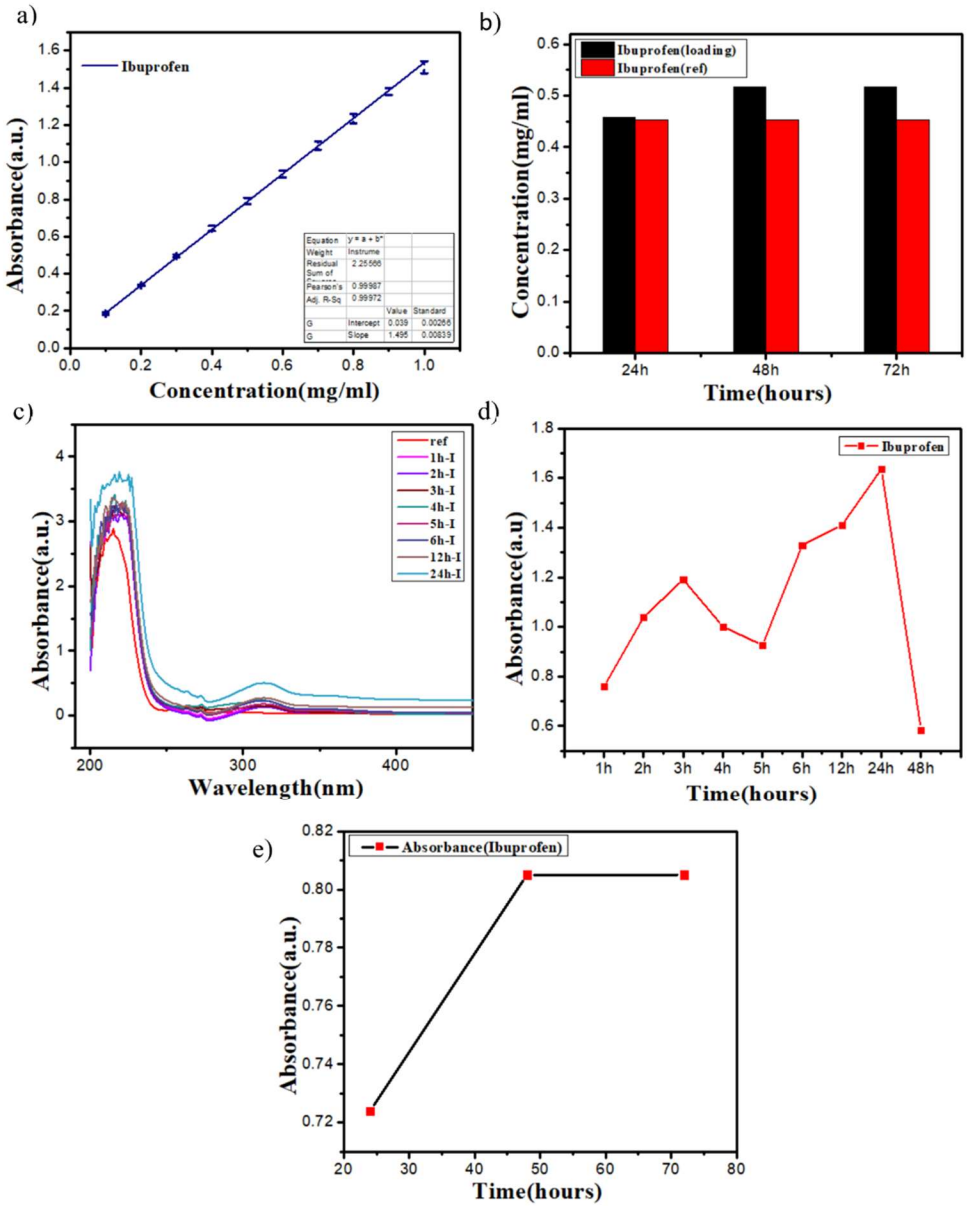

Figure 17: a) The relation between concentration and absorbance of ibuprofen, b) Concentration of ibuprofen loaded at 24 hours, 48 hours, and 72 hours, c) **UV-Vis** spectra of **ibuprofen** during drug loading, d) **Linearity plot** of ibuprofen drug loading for **48 hours**, e) **Linearity plot** of ibuprofen drug loading for **72 hours**.

4.3.3 Data of Curcumin Loading

UV-Vis data confirms that the loading occurred between 24 hours and 48 hours.

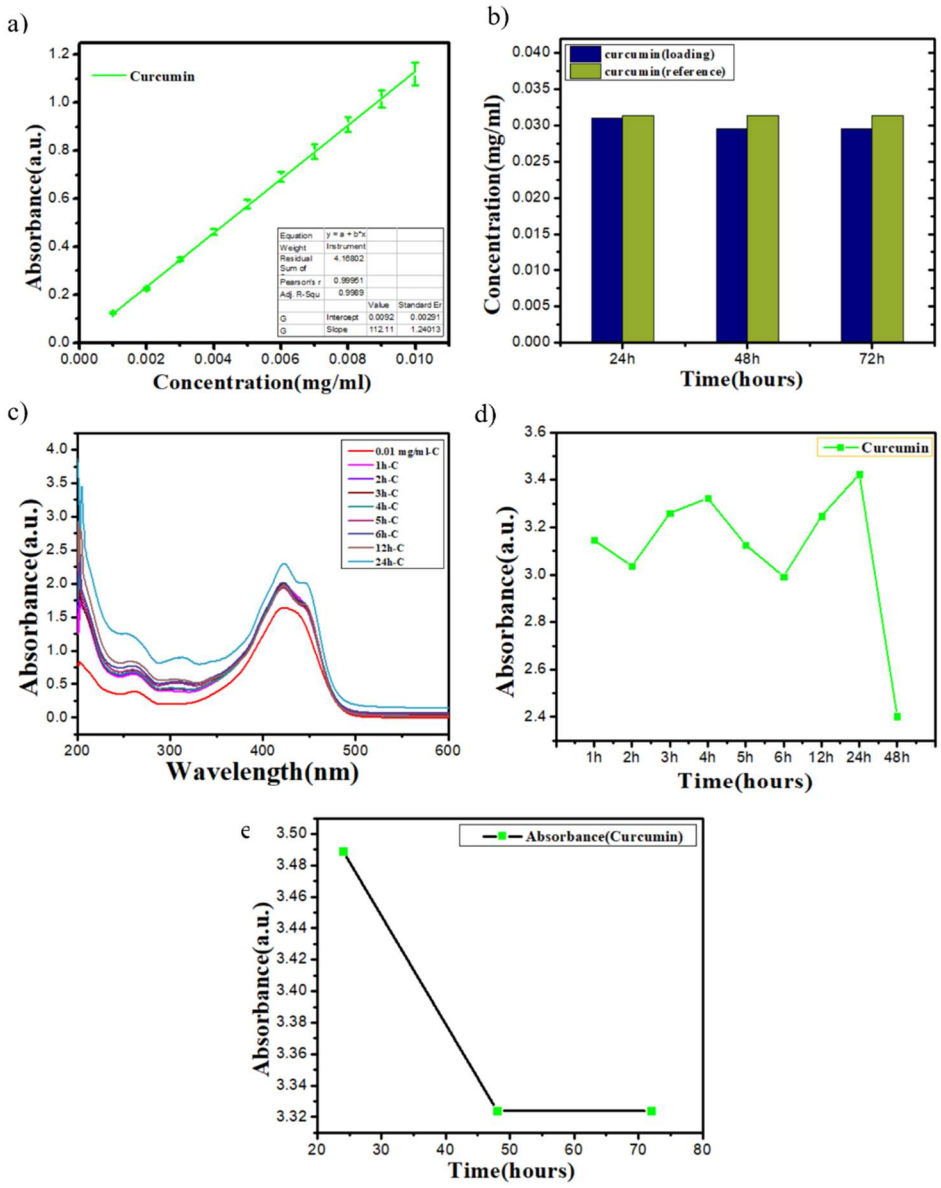

Figure 18: a) The relation between concentration and absorbance of curcumin, b) Concentration of curcumin loaded at 24 hours, 48 hours, and 72 hours, c) **UV-Vis** spectra of **curcumin** during drug loading, d) **Linearity plot** of curcumin drug loading for **48 hours**, e) **Linearity plot** of curcumin drug loading for **72 hours**.

4.4 Data of Drug Release Experiments

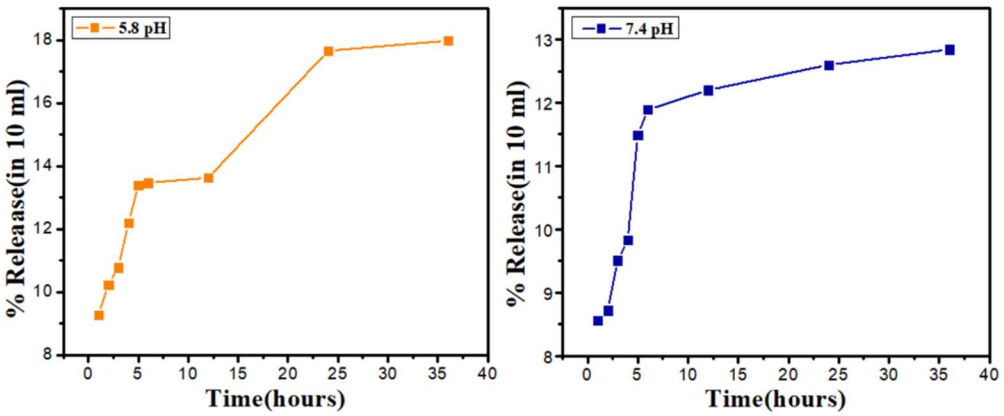

Figure 19: Relation between % drug release and time in 5.8 and 7.4 pH DI water solution after Curcumin drug release experiment.

Chapter 5

Conclusion and Future Scope

Our study underscores the promising role of copper-based MOFs, particularly **IITI-3**, in biomedical applications, particularly drug delivery. Through a comprehensive characterization process involving PXRD, TGA, BET, IR, and UV techniques, we have demonstrated the efficacy of **IITI-3** as a versatile carrier for drug molecules. Our findings highlight its high loading capacities, precision tunability, and ability to accommodate multiple drugs simultaneously.

Moreover, our investigation into the delivery of Ibuprofen and Curcumin reveals intriguing insights. While both drugs could be loaded into **IITI-3** concurrently, selective encapsulation was observed, with only Curcumin being individually encapsulated. This selectivity suggests the potential for targeted drug delivery strategies utilizing **IITI-3**, particularly in pH-responsive environments such as tumor microenvironments.

Furthermore, our pH-dependent release studies, conducted under physiological and second intestine pH, further validate the suitability of **IITI-3** for targeted drug administration. The pH-responsive behavior exhibited by **IITI-3** holds promise for applications where precise control over drug release is essential, particularly in conditions mimicking tumor microenvironments.

In essence, the findings presented here contribute to the growing body of evidence supporting the utility of MOFs in biomedical applications, paving the way for future advancements in targeted drug, protein, gene delivery and therapeutic interventions.

REFERENCES

1. Patra, J.K.; Das, G.; Fraceto, L.F.; Campos, E.V.R.; del Pilar Rodriguez-Torres, M.; Acosta-Torres, L.S.; Diaz-Torres, L.A.; Grillo, R.;Swamy, M.K.; Sharma, S.; et al. Nano based drug delivery systems: Recent developments and future prospects. *J. Nanobiotechnol*. **2018**, *16*, 71.
2. Meng, L.; Zhang, X.; Lu, Q.; Fei, Z.; Dyson, P.J. Single walled carbon nanotubes as drug delivery vehicles: Targeting doxorubicin to tumors. *Biomaterials* **2012**, 33, 1689–1698.
3. Chamundeeswari, M.; Jeslin, J.; Verma, M.L. Nanocarriers for drug delivery applications. *Environ. Chem. Lett*. **2018**, *17*, 849–865.
4. Erttmann, R.; Erb, N.; Steinhoff, A.; Landbeck, G. Pharmacokinetics of doxorubicin in man: Dose and schedule dependence. *J. Cancer Res. Clin. Oncol.* **1988**, *114*, 509–513.
5. Shan, K. Anthracycline-Induced Cardiotoxicity. *Ann. Intern. Med*. **1996**, *125*, 47.
6. Din, F.; Aman, W.; Ullah, I.; Qureshi, O.S.; Mustapha, O.; Shafique, S.; Zeb, A. Effective use of nanocarriers as drug delivery systems for the treatment of selected tumors. *Int. J. Nanomed*. **2017**, *12*, 7291–7309.
7. Orellana-Tavra, C.; Baxter, E.F.; Tian, T.; Bennett, T.D.; Slater, N.K.H.; Cheetham, A.K.; Fairen-Jimenez, D. Amorphous metal–organic frameworks for drug delivery. *Chem. Commun*. **2015**, *51*, 13878–13881.
8. Martinho, N.; Damgé, C.; Reis, C.P. Recent Advances in Drug Delivery Systems. *J. Biomater. Nanobiotechnol*. **2011**, *02*, 510–526.
9. Baskar, G.; Bikku George, G.; Chamundeeswari, M. Synthesis and Characterization of Asparaginase Bound Silver Nanocomposite Against Ovarian Cancer Cell Line A2780 and Lung Cancer Cell Line A549. *J. Inorg. Organomet. Polym. Mater*. **2016**, *27*, 87–94.
10. Baskar, G.; Lalitha, K.; Garrick, B.G.; Chamundeeswari, M. *Conjugation, Labeling and Characterization of Asparaginase Bound Silver Nanoparticles for Anticancer Applications*; NISCAIR-CSIR: New Delhi, India, **2017**; Volume 55.
11. Muthukumar, T.; Chamundeeswari, M.; Prabhavathi, S.; Gurunathan, B.; Chandhuru, J.; Sastry, T.P. Carbon nanoparticle from a natural source fabricated for folate receptor

targeting, imaging and drug delivery application in A549 lung cancer cells. *Eur. J. Pharm. Biopharm*. **2014**, *88*, 730–736.

12. Vauthier, C.; Labarre, D.; Ponchel, G. Design aspects of poly(alkylcyanoacrylate) nanoparticles for drug delivery. *J. Drug Target*. **2007**, *15*, 641–663.
13. Chamundeeswari, M.; Sastry, T.P.; Lakhsmi, B.S.; Senthil, V.; Agostinelli, E. Iron nanoparticles from animal blood for cellular imaging and targeted delivery for cancer treatment. *Biochim. Biophys. Acta-Gen. Subj*. **2013**, *1830*, 3005–3010.
14. Gelperina, S.; Kisich, K.; Iseman, M.D.; Heifets, L. The Potential Advantages of Nanoparticle Drug Delivery Systems in Chemotherapy of Tuberculosis. *Am. J. Respir. Crit. Care Med*. **2005**, *172*, 1487–1490.
15. Baskar, G.; Garrick, B.G.; Lalitha, K.; Chamundeeswari, M. Gold nanoparticle mediated delivery of fungal asparaginase against cancer cells. *J. Drug Deliv. Sci. Technol*. **2018**, *44*, 498–504.
16. Rebekah, A.; Sivaselvam, S.; Viswanathan, C.; Prabhu, D.; Gautam, R.; Ponpandian, N. Magnetic nanoparticle-decorated graphene oxide-chitosan composite as an efficient nanocarrier for protein delivery. *Colloids Surf. A Physicochem. Eng. Asp*. **2021**, *610*, 125913.
17. Luzuriaga, M.A.;Welch, R.P.; Dharmarwardana, M.; Benjamin, C.E.; Li, S.; Shahrivarkevishahi, A.; Popal, S.; Tuong, L.H.; Creswell, C.T.; Gassensmith, J.J. Enhanced Stability and Controlled Delivery of MOF-Encapsulated Vaccines and Their Immunogenic Response In Vivo. *ACS Appl. Mater. Interfaces* **2019**, *11*, 9740–9746.
18. Kabanov, A.V.; Lemieux, P.; Vinogradov, S.; Alakhov, V. Pluronic®block copolymers: Novel functional molecules for gene therapy. *Adv. Drug Deliv. Rev*. **2002**, *54*, 223–233.
19. Verma, M.L.; Barrow, C.J.; Puri, M. Nanobiotechnology as a novel paradigm for enzyme immobilisation and stabilisation with potential applications in biodiesel production. *Appl. Microbiol. Biotechnol*. **2012**, *97*, 23–39.
20. Neubert, R.H.H. Potentials of new nanocarriers for dermal and transdermal drug delivery. *Eur. J. Pharm. Biopharm*. **2011**, *77*, 1–2.
21. Jahangirian, H.; Ghasemian Lemraski, E.; Webster, T.J.; Rafiee-Moghaddam, R.; Abdollahi, Y. A review of drug delivery systems based on nanotechnology and green chemistry: Green nanomedicine. *Int. J. Nanomed*. **2017**, *12*, 2957–2978.

22. de Villiers, M.M.; Aramwit, P.; Kwon, G.S. Nanotechnology in Drug Delivery; de Villiers, M.M., Aramwit, P., Kwon, G.S., Eds.; Springer: New York, NY, USA, **2009**; Volume 10.
23. Mirza, A.Z.; Siddiqui, F.A. Nanomedicine and drug delivery: A mini review. *Int. Nano Lett*. **2014**, *4*, 94.
24. Lu, H.; Wang, J.; Wang, T.; Zhong, J.; Bao, Y.; Hao, H. Recent Progress on Nanostructures for Drug Delivery Applications. *J. Nanomater*. **2016**, *2016*, 5762431.
25. Ding, S.; Khan, A.I.; Cai, X.; Song, Y.; Lyu, Z.; Du, D.; Dutta, P.; Lin, Y. Overcoming blood–brain barrier transport: Advances in nanoparticle-based drug delivery strategies. *Mater. Today* **2020**, *37*, 112–125.
26. López-Dávila, V.; Seifalian, A.M.; Loizidou, M. Organic nanocarriers for cancer drug delivery. *Curr. Opin. Pharmacol*. **2012**, *12*, 414–419.
27. Santos, H.A.; Bimbo, L.M.; Peltonen, L.; Hirvonen, J. Inorganic Nanoparticles in Targeted Drug Delivery and Imaging. In Targeted Drug Delivery: *Concepts and Design*; Springer: Cham, Switzerland, **2014**; pp. 571–613.
28. Karami, A.; Mohamed, O.; Ahmed, A.; Husseini, G.A.; Sabouni, R. Recent Advances in Metal-Organic Frameworks as Anticancer Drug Delivery Systems: A Review. *Anti-Cancer Agents Med. Chem*. **2021**, *21*, 2487–2504.
29. Qian, W.Y.; Sun, D.M.; Zhu, R.R.; Du, X.L.; Liu, H.; Wang, S.L. pH-sensitive strontium carbonate nanoparticles as new anticancer vehicles for controlled etoposide release. *Int. J. Nanomed*. **2012**, *7*, 5781.
30. Sun, T.; Zhang, Y.S.; Pang, B.; Hyun, D.C.; Yang, M.; Xia, Y. Engineered Nanoparticles for Drug Delivery in Cancer Therapy. *Angew. Chem. Int. Ed*. 2014, *126*, 12520–12568.
31. Mishra, B.; Patel, B.B.; Tiwari, S. Colloidal nanocarriers: A review on formulation technology, types and applications toward targeted drug delivery. *Nanomed. Nanotechnol. Biol. Med*. **2010**, *6*, 9–24.
32. Soppimath, K.S.; Aminabhavi, T.M.; Kulkarni, A.R.; Rudzinski,W.E. Biodegradable polymeric nanoparticles as drug delivery devices. *J. Control. Release* **2001**, *70*, 1–20.
33. Ochekpe, N.A.; Olorunfemi, P.O.; Ngwuluka, N.C. Nanotechnology and Drug Delivery Part 2: Nanostructures for Drug Delivery. *Trop. J. Pharm. Res*. **2009**, 8.
34. Meng, F.; Zhong, Z.; Feijen, J. Stimuli-Responsive Polymersomes for Programmed Drug Delivery. *Biomacromolecules* **2009**, *10*, 197–209.

35. Lim, H.J.; Cho, E.C.; Shim, J.; Kim, D.-H.; An, E.J.; Kim, J. Polymer-associated liposomes as a novel delivery system for cyclodextrin-bound drugs. *J. Colloid Interface Sci*. **2008**, *320*, 460–468.
36. Korting, H.C.; Schäfer-Korting, M. Carriers in the Topical Treatment of Skin Disease. *Drug Deliv*. **2009**, *197*, 435–468.
37. Schaffazick, S.R.; Pohlmann, A.R.; de Cordova, C.A.S.; Creczynski-Pasa, T.B.; Guterres, S.S. Protective properties of melatoninloaded nanoparticles against lipid peroxidation. *Int. J. Pharm*. **2005**, *289*, 209–213.
38. Castro, G.A.; Oréfice, R.L.; Vilela, J.M.C.; Andrade, M.S.; Ferreira, L.A.M. Development of a new solid lipid nanoparticle formulation containing retinoic acid for topical treatment of acne. *J. Microencapsul*. **2007**, *24*, 395–407.
39. Fornaguera C, Solans C. Methods for the in vitro characterization of nanomedicines—biological component interaction. *J Pers Med.* **2017**,*7*,1–16.
40. Grabska-Zieli ´nska, S.; Sionkowska, A.; Carvalho, Â.; Monteiro, F.J. Biomaterials with Potential Use in Bone Tissue Regeneration —Collagen/Chitosan/Silk Fibroin Scaffolds Cross-Linked by EDC/NHS. *Materials.* **2021**, *14*, 1105.
41. VectorStock (2024), www.vectorstock.com
42. Huda, S.; Alam, M.A.; Sharma, P.K. Smart nanocarriers-based drug delivery for cancer therapy: An innovative and developing strategy. *J. Drug Deliv. Sci. Technol*. **2020**, *60*, 102018.
43. Bhatia, S. Nanoparticles types, classification, characterization, fabrication methods and drug delivery applications. *In Natural Polymer Drug Delivery Systems*; Springer: Cham, Switzerland, **2016**; pp. 33–93.
44. Ghezzi, M.; Pescina, S.; Padula, C.; Santi, P.; Del Favero, E.; Cantù, L.; Nicoli, S. Polymeric micelles in drug delivery: An insight of the techniques for their characterization and assessment in biorelevant conditions. *J. Control. Release* **2021**, *332*, 312–336.
45. Geißler, D.; Charbonnière, L.J.; Ziessel, R.F.; Butlin, N.G.; Löhmannsröben, H.-G.; Hildebrandt, N. Quantum Dot Biosensors for Ultrasensitive Multiplexed Diagnostics. Angew. *Chem. Int. Ed*. **2010**, *49*, 1396–1401.

46. Hossen, S.; Hossain, M.K.; Basher, M.K.; Mia, M.N.H.; Rahman, M.T.; Uddin, M.J. Smart nanocarrier-based drug delivery systems for cancer therapy and toxicity studies: A review. *J. Adv. Res*. **2019**, *15*, 1–18.
47. Li, B.; Wen, H.-M.; Cui, Y.; Zhou, W.; Qian, G.; Chen, B. Emerging Multifunctional Metal-Organic Framework Materials. *Adv. Mater*. **2016**, *28*, 8819–8860.
48. Nandasiri, M.I.; Jambovane, S.R.; McGrail, B.P.; Schaef, H.T.; Nune, S.K. Adsorption, separation, and catalytic properties of densified metal-organic frameworks. *Coord. Chem. Rev*. **2016**, *311*, 38–52.
49. Furukawa, H.; Cordova, K.E.; O'Keeffe, M.; Yaghi, O.M. The Chemistry and Applications of Metal-Organic Frameworks. *Science* **2013**, *341*, 1230444.
50. Zhang, S.; Pei, X.; Gao, H.; Chen, S.;Wang, J. Metal-organic framework-based nanomaterials for biomedical applications. *Chin. Chem. Lett*. **2020**, *31*, 1060–1070.
51. Eddaoudi, M. Systematic Design of Pore Size and Functionality in Isoreticular MOFs and Their Application in Methane Storage. *Science* **2002**, *295*, 469–472.
52. Suh, M.P.; Park, H.J.; Prasad, T.K.; Lim, D.-W. Hydrogen Storage in Metal–Organic Frameworks. *Chem. Rev.* **2011**, *112*, 782–835.
53. Chen, B.; Xiang, S.; Qian, G. Metal□Organic Frameworks with Functional Pores for Recognition of Small Molecules. *Acc. Chem. Res*. **2010**, *43*, 1115–1124.
54. Li, S.; Huo, F. Metal–organic framework composites: From fundamentals to applications. *Nanoscale* **2015**, *7*, 7482–7501.
55. Zhang, Y.; Yang, L.; Yan, L.;Wang, G.; Liu, A. Recent advances in the synthesis of spherical and nanoMOF-derived multifunctional porous carbon for nanomedicine applications. *Coord. Chem. Rev*. **2019**, *391*, 69–89.
56. Lee, J.; Farha, O.K.; Roberts, J.; Scheidt, K.A.; Nguyen, S.T.; Hupp, J.T. Metal–organic framework materials as catalysts. *Chem. Soc. Rev*. **2009**, *38*, 1450.
57. Li, Z.; Peters, A.W.; Platero-Prats, A.E.; Liu, J.; Kung, C.-W.; Noh, H.; DeStefano, M.R.; Schweitzer, N.M.; Chapman, K.W.; Hupp, J.T.; et al. Fine-Tuning the Activity of Metal–Organic Framework-Supported Cobalt Catalysts for the Oxidative Dehydrogenation of Propane. *J. Am. Chem. Soc*. **2017**, *139*, 15251–15258.
58. Al Sharabati, M.; Sabouni, R. Selective removal of dual dyes from aqueous solutions using a metal organic framework (MIL-53(Al)). *Polyhedron* **2020**, *190*, 114762.

59. Schoedel, A.; Ji, Z.; Yaghi, O.M. The role of metal–organic frameworks in a carbon-neutral energy cycle. *Nat. Energy* **2016**, *1*.
60. Zhang, T.; Lin, W. Metal–organic frameworks for artificial photosynthesis and photocatalysis. *Chem. Soc. Rev*. **2014**, *43*, 5982–5993.
61. Lian, X.; Fang, Y.; Joseph, E.; Wang, Q.; Li, J.; Banerjee, S.; Lollar, C.; Wang, X.; Zhou, H.-C. Enzyme–MOF (metal–organic framework) composites. *Chem. Soc. Rev*. **2017**, *46*, 3386–3401.
62. Feng, L.;Wang, K.Y.; Lv, X.L.; Yan, T.H.; Zhou, H.C. Hierarchically porous metal-organic frameworks: Synthetic strategies and applications. *Natl. Sci. Rev*. **2020**, *7*, 1743–1758.
63. An, H.; Li, M.; Gao, J.; Zhang, Z.; Ma, S.; Chen, Y. Incorporation of biomolecules in Metal-Organic Frameworks for advanced applications. *Coord. Chem. Rev*. **2019**, *384*, 90–106.
64. Malik, P.; Gupta, R.; Ameta, R.K. Unique attributes of metal-organic frameworks in drug delivery. *In Metal-Organic Frameworks for Chemical Reactions*; Elsevier: Amsterdam, The Netherlands, **2021**; pp. 389–415.
65. Sun, Y.; Zheng, L.; Yang, Y.; Qian, X.; Fu, T.; Li, X.; Yang, Z.; Yan, H.; Cui, C.; Tan, W. Metal–Organic Framework Nanocarriers for Drug Delivery in Biomedical Applications. *Nano-Micro Lett*. **2020**, 12.
66. Anand, R.; Borghi, F.; Manoli, F.; Manet, I.; Agostoni, V.; Reschiglian, P.; Gref, R.; Monti, S. Host–Guest Interactions in Fe(III)- Trimesate MOF Nanoparticles Loaded with Doxorubicin. *J. Phys. Chem. B* **2014**, *118*, 8532–8539.
67. Bunzen, H.; Grzywa, M.; Hambach, M.; Spirkl, S.; Volkmer, D. From Micro to Nano: A Toolbox for Tuning Crystal Size and Morphology of Benzotriazolate-Based Metal-Organic Frameworks. *Cryst. Growth Des*. **2016**, *16*, 3190–3197.
68. Schwirn, K.; Tietjen, L.; Beer, I. Why are nanomaterials different and how can they be appropriately regulated under REACH? *Environ. Sci. Eur*. **2014**, *26*, 4.
69. Głowniak, S.; Szcz¸e´sniak, B.; Choma, J.; Jaroniec, M. Mechanochemistry: Toward green synthesis of metal–organic frameworks. *Mater. Today* **2021**, *46*, 109–124.
70. Lee, Y.-R.; Kim, J.; Ahn,W.-S. Synthesis of metal-organic frameworks: A mini review. *Korean J. Chem. Eng*. **2013**, *30*, 1667–1680.

71. Chen, X.-Y.; Zhao, B.; Shi, W.; Xia, J.; Cheng, P.; Liao, D.-Z.; Yan, S.-P.; Jiang, Z.-H. Microporous Metal□Organic Frameworks Built on a Ln3Cluster as a Six-Connecting *Node. Chem. Mater*. **2005**, *17*, 2866–2874.
72. Wang, D.; He, H.; Chen, X.; Feng, S.; Niu, Y.; Sun, D. A 3D porous metal–organic framework constructed of 1D zigzag and helical chains exhibiting selective anion exchange. *CrystEngComm* **2010**, *12*, 1041–1043.
73. Mueller, U.; Schubert, M.; Teich, F.; Puetter, H.; Schierle-Arndt, K.; Pastré, J. Metal–organic frameworks—prospective industrial applications. *J. Mater. Chem*. **2006**, *16*, 626–636.
74. Campagnol, N.; Souza, E.R.; De Vos, D.E.; Binnemans, K.; Fransaer, J. Luminescent terbium-containing metal–organic framework films: New approaches for the electrochemical synthesis and application as detectors for explosives. *Chem. Commun*. **2014**, *50*, 12545–12547.
75. Phang,W.J.; Lee,W.R.; Yoo, K.; Ryu, D.W.; Kim, B.; Hong, C.S. pH-Dependent Proton Conducting Behavior in a Metal-Organic Framework Material. *Angew. Chem. Int. Ed*. **2014**, *53*, 8383–8387.
76. Sabouni, R.; Kazemian, H.; Rohani, S. Microwave Synthesis of the CPM-5 Metal Organic Framework. *Chem. Eng. Technol*. **2012**, *35*, 1085–1092.
77. Babu, R.; Roshan, R.; Kathalikkattil, A.C.; Kim, D.W.; Park, D.W. Rapid, Microwave-Assisted Synthesis of Cubic, Three-Dimensional, Highly Porous MOF-205 for Room Temperature CO2 Fixation via Cyclic Carbonate Synthesis. *ACS Appl. Mater. Interfaces* **2016**, *8*, 33723–33731.
78. Pichon, A.; Lazuen-Garay, A.; James, S.L. Solvent-free synthesis of a microporous metal–organic framework. *CrystEngComm* **2006**, *8*, 211.
79. Masoomi, M.Y.; Morsali, A.; Junk, P.C. Rapid mechanochemical synthesis of two new Cd(ii)-based metal–organic frameworks with high removal efficiency of Congo red. *CrystEngComm* **2015**, *17*, 686–692.
80. Qiu, S.; Zhu, G. Molecular engineering for synthesizing novel structures of metal–organic frameworks with multifunctional properties. *Coord. Chem. Rev*. **2009**, *253*, 2891–2911.

81. Shen, L.;Wu,W.; Liang, R.; Lin, R.;Wu, L. Highly dispersed palladium nanoparticles anchored on UiO-66(NH2) metal-organic framework as a reusable and dual functional visible-light-driven photocatalyst. *Nanoscale* **2013**, *5*, 9374.
82. Morsali, A.; Monfared, H.H.; Morsali, A.; Janiak, C. Ultrasonic irradiation assisted syntheses of one-dimensional di(azido)- dipyridylamine Cu(II) coordination polymer nanoparticles. *Ultrason. Sonochem*. **2015**, *23*, 208–211.
83. Hwang, Y.K.; Chang, J.-S.; Park, S.-E.; Kim, D.S.; Kwon, Y.-U.; Jhung, S.H.; Hwang, J.-S.; Park, M.S. Microwave Fabrication of MFI Zeolite Crystals with a Fibrous Morphology and Their Applications. *Angew. Chem. Int. Ed*. **2005**, *44*, 556–560.
84. Trong On, D.; Nguyen, S.V.; Hulea, V.; Dumitriu, E.; Kaliaguine, S. Mono- and bifunctional MFI, BEA and MCM-41 titaniummolecular sieves. Part 1. Synthesis and characterization. *Microporous Mesoporous Mater*. **2003**, *57*, 169–180.
85. Kang, K.K.; Park, C.H.; Ahn,W.S. Microwave preparation of a titanium-substituted mesoporous molecular sieve. *Catal. Lett*. **1999**, *59*, 45–49.
86. Kaupp, G. Mechanochemistry: The varied applications of mechanical bond-breaking. *CrystEngComm* **2009**, *11*, 388–403.
87. Garay, A.L.; Pichon, A.; James, S.L. Solvent-free synthesis of metal complexes. *Chem. Soc. Rev*. **2007**, *36*, 846.
88. George, P.; Das, R.K.; Chowdhury, P. Facile microwave synthesis of Ca-BDC metal organic framework for adsorption and controlled release of Curcumin. *Microporous Mesoporous Mater*. **2019**, *281*, 161–171.
89. Xu, H.; Zeiger, B.W.; Suslick, K.S. Sonochemical synthesis of nanomaterials. *Chem. Soc. Rev*. **2013**, *42*, 2555–2567.
90. Dai, S.; Nouar, F.; Zhang, S.; Tissot, A.; Serre, C. One-Step Room-Temperature Synthesis of Metal(IV) Carboxylate Metal—Organic Frameworks. *Angew. Chem. Int. Ed*. **2021**, *60*, 4282–4288.
91. Getachew, N.; Chebude, Y.; Diaz, I.; Sanchez-Sanchez, M. Room temperature synthesis of metal organic framework MOF-2. *J. Porous Mater*. **2014**, *21*, 769–773.
92. Tranchemontagne, D.J.; Hunt, J.R.; Yaghi, O.M. Room temperature synthesis of metal-organic frameworks: MOF-5, MOF-74, MOF-177, MOF-199, and IRMOF-0. *Tetrahedron* **2008**, *64*, 8553–8557.

93. Bang, J.H.; Suslick, K.S. Applications of Ultrasound to the Synthesis of Nanostructured Materials. *Adv. Mater*. **2010**, *22*, 1039–1059.
94. Ahmadi, M.; Ayyoubzadeh, S.M.; Ghorbani-Bidkorbeh, F.; Shahhosseini, S.; Dadashzadeh, S.; Asadian, E.; Mosayebnia, M.; Siavashy, S. An investigation of affecting factors on MOF characteristics for biomedical applications: A systematic review. *Heliyon* **2021**, *7*, e06914.
95. Sajid, M.; Ihsanullah. Toxicity of nanoscale metal-organic frameworks in biological systems. In Metal-Organic Frameworks for Biomedical Applications; Woodhead Publishing: *Sawston, UK*, **2020**; pp. 383–395.
96. Simon-Yarza, T.; Mielcarek, A.; Couvreur, P.; Serre, C. Nanoparticles of Metal-Organic Frameworks: On the Road to In Vivo Efficacy in Biomedicine. *Adv. Mater*. **2018**, *30*, 1707365.
97. Sun, C.Y.; Qin, C.;Wang, C.G.; Su, Z.M.; Wang, S.; Wang, X.L.; Yang, G.S.; Shao, K.Z.; Lan, Y.Q.;Wang, E.B. Chiral Nanoporous Metal-Organic Frameworks with High Porosity as Materials for Drug Delivery. *Adv. Mater*. **2011**, *23*, 5629–5632.
98. He, S.; Wu, L.; Li, X.; Sun, H.; Xiong, T.; Liu, J.; Huang, C.; Xu, H.; Sun, H.; Chen, W.; et al. Metal-organic frameworks for advanced drug delivery. *Acta Pharm. Sin. B* **2021**, *11*, 2362–2395.
99. Sun, K.; Li, L.; Yu, X.L.; Liu, L.; Meng, Q.; Wang, F.; Zhang, R. Functionalization of mixed ligand metal-organic frameworks as the transport vehicles for drugs. *J. Colloid Interface Sci*. **2017**, *486*, 128–135.
100. Leng, X.; Dong, X.;Wang,W.; Sai, N.; Yang, C.; You, L.; Huang, H.; Yin, X.; Ni, J. Biocompatible Fe-Based Micropore Metal-Organic Frameworks as Sustained-Release Anticancer Drug Carriers. *Molecules* **2018**, *23*, 2490.
101. Sun, C.Y.; Qin, C.; Wang, X.L.; Yang, G.S.; Shao, K.Z.; Lan, Y.Q.; Su, Z.M.; Huang, P.; Wang, C.G.; Wang, E.B. Zeolitic imidazolate framework-8 as efficient pH-sensitive drug delivery vehicle. *Dalt. Trans*. **2012**, *41*, 6906–6909.
102. Gao, H.; Zhang, Y.; Chi, B.; Lin, C.; Tian, F.; Xu, M.; Wang, Y.; Xu, Z.; Li, L.; Wang, J. Synthesis of 'dual-key-and-lock' drug carriers for imaging and improved drug release. *Nanotechnology* **2020**, *31*, 445102.

103. Rao, S.; Chen, R.; LaRocca, A.A.; *et al.* Remotely controlled chemomagnetic modulation of targeted neural circuits. *Nat. Nanotechnol.* **2019**,*14*, 967–973.

104. wikipedia (2024), en.wikipedia.org

105. S. Cho.; Zaslavsky A.; Richter C.A.; Majikes J. M.; Kiddle J. A.; Andrieu F.; Barraud S.; Balijepalli A.; High-Resolution DNA Binding Kinetics Measurements with Double Gate FD-SOI Transistors, *International Electron Devices Meeting (IEDM)*, **2022**,*24*,1-4s

106. Ferrari, M. Cancer nanotechnology: Opportunities and challenges. *Nat. Rev. Cancer* **2005**, *5*, 161–171.

107. Fattal, E.; Grabowski, N.; Mura, S.; Vergnaud, J.; Tsapis, N.; Hillaireau, H. Lung Toxicity of Biodegradable Nanoparticles. *J. Biomed. Nanotechnol*. **2014**, *10*, 2852–2864.

108. Mitragotri, S.; Burke, P.A.; Langer, R. Overcoming the challenges in administering biopharmaceuticals: Formulation and delivery strategies. *Nat. Rev. Drug Discov*. **2014**, *13*, 655–672.

109. Furukawa, S.; Reboul, J.; Diring, S.; Sumida, K.; Kitagawa, S. Structuring of metal–organic frameworks at the mesoscopic/ macroscopic scale. *Chem. Soc. Rev*. **2014**, *43*, 5700–5734.

110. Wang, D.; Jana, D.; Zhao, Y. Metal-Organic Framework Derived Nanozymes in Biomedicine. *Acc. Chem. Res*. **2020**, *53*, 1389–1400.

111. Wu, Y.; Darland, D.C.; Zhao, J.X. Nanozymes—Hitting the Biosensing "Target". *Sensors* **2021**, *21*, 5201.

112. Banerjee, S.; Lollar, C.T.; Xiao, Z.; Fang, Y.; Zhou, H.C. Biomedical Integration of Metal–Organic Frameworks. *Trends Chem*. **2020**, *2*, 467–479.

113. Zhang, X.; Fang, L.; Jiang, K.; He, H.; Yang, Y.; Cui, Y.; Li, B.; Qian, G. Nanoscale fluorescent metal–organic framework composites as a logic platform for potential diagnosis of asthma. *Biosens. Bioelectro*n. **2019**, *130*, 65–72.

114. Jiang, P.; Hu, Y.; Li, G. Biocompatible Au@Ag nanorod@ZIF-8 core-shell nanoparticles for surface-enhanced Raman scattering imaging and drug delivery. *Talanta* **2019**, *200*, 212–217.

115. Taylor-Pashow, K.M.L.; Della Rocca, J.; Xie, Z.; Tran, S.; Lin, W. Postsynthetic Modifications of Iron-Carboxylate Nanoscale Metal□Organic Frameworks for Imaging and Drug Delivery. *J. Am. Chem. Soc*. **2009**, *131*, 14261–14263.

116. Lu, K.; He, C.; Lin, W. Nanoscale Metal–Organic Framework for Highly Effective Photodynamic Therapy of Resistant Head and Neck Cancer. *J. Am. Chem. Soc*. **2014**, *136*, 16712–16715.

117. Shi, Z.; Chu, C.; Zhang, Y.; Su, Z.; Lin, H.; Pang, X.;Wang, X.; Liu, G.; Li,W. Self-Assembled Metal-Organic Nanoparticles for Multimodal Imaging-Guided Photothermal Therapy of Hepatocellular Carcinoma. *J. Biomed. Nanotechnol*. **2018**, *14*, 1934–1943.

118. Kundu, T.; Mitra, S.; DíazDíaz, D.; Banerjee, R. Gadolinium(III)-Based Porous Luminescent Metal-Organic Frameworks for Bimodal Imaging. *Chempluschem* **2016**, *81*, 728–732.

119. Zhang, T.;Wang, L.; Ma, C.;Wang,W.; Ding, J.; Liu, S.; Zhang, X.; Xie, Z. BODIPY-containing nanoscale metal–organic frameworks as contrast agents for computed tomography. *J. Mater. Chem. B* **2017**, *5*, 2330–2336.

120. Cai, W.; Gao, H.; Chu, C.; Wang, X.; Wang, J.; Zhang, P.; Lin, G.; Li, W.; Liu, G.; Chen, X. Engineering Phototheranostic Nanoscale Metal–Organic Frameworks for Multimodal Imaging-Guided Cancer Therapy. *ACS Appl. Mater. Interfaces* **2017**, *9*, 2040–2051.

121. Ma, W.; Jiang, Q.; Yu, P.; Yang, L.; Mao, L. Zeolitic Imidazolate Framework-Based Electrochemical Biosensor for in Vivo Electrochemical Measurements. *Anal. Chem*. **2013**, *85*, 7550–7557.

122. Millward, A.R.; Yaghi, O.M. Metal□Organic Frameworks with Exceptionally High Capacity for Storage of Carbon Dioxide at Room Temperature. *J. Am. Chem. Soc*. **2005**, *127*, 17998–17999.

123. Xu, R.; Wang, Y.; Duan, X.; Lu, K.; Micheroni, D.; Hu, A.; Lin, W. Nanoscale Metal–Organic Frameworks for Ratiometric Oxygen Sensing in Live Cells. *J. Am. Chem. Soc*. **2016**, *138*, 2158–2161.

124. deKrafft, K.E.; Boyle,W.S.; Burk, L.M.; Zhou, O.Z.; Lin,W. Zr- and Hf-based nanoscale metal–organic frameworks as contrast agents for computed tomography. *J. Mater. Chem*. **2012**, *22*, 18139.

125. Zhao, D.; Zhang, J.; Yue, D.; Lian, X.; Cui, Y.; Yang, Y.; Qian, G. A highly sensitive near-infrared luminescent metal–organic framework thermometer in the physiological range. *Chem. Commun*. **2016**, *52*, 8259–8262.

126. Zhang, J.-W.; Zhang, H.-T.; Du, Z.-Y.; Wang, X.; Yu, S.-H.; Jiang, H.-L. Water-stable metal–organic frameworks with intrinsic peroxidase-like catalytic activity as a colorimetric biosensing platform. *Chem. Commun*. **2014**, *50*, 1092–1094.

127. Liu, M.; Du, H.; Zhang,W.; Zhai, G. Internal stimuli-responsive nanocarriers for drug delivery: Design strategies and applications. *Mater. Sci. Eng. C* **2017**, *71*, 1267–1280.

128. Ganta, S.; Devalapally, H.; Shahiwala, A.; Amiji, M. A review of stimuli-responsive nanocarriers for drug and gene delivery. *J. Control. Release* **2008**, *126*, 187–204.

129. Kang, T.; Li, F.; Baik, S.; Shao, W.; Ling, D.; Hyeon, T. Surface design of magnetic nanoparticles for stimuli-responsive cancer imaging and therapy. *Biomaterials* **2017**, *136*, 98–114.

130. Zhang, Y.; Yu, J.; Bomba, H.N.; Zhu, Y.; Gu, Z. Mechanical Force-Triggered Drug Delivery. *Chem. Rev*. **2016**, *116*, 12536–12563.

131. Qu, J.;Wang, Q.Y.; Chen, K.L.; Luo, J.B.; Zhou, Q.H.; Lin, J. Reduction/temperature/pH multi-stimuli responsive core cross-linked polypeptide hybrid micelles for triggered and intracellular drug release. *Colloids Surf. B Biointerfaces* **2018**, *170*, 373–381.

132. Liu, J.; Pang, Y.; Zhu, Z.;Wang, D.; Li, C.; Huang,W.; Zhu, X.; Yan, D. Therapeutic nanocarriers with hydrogen peroxide-triggered drug release for cancer treatment. *Biomacromolecules* **2013**, *14*, 1627–1636.

133. Wang, H.S. Metal–organic frameworks for biosensing and bioimaging applications. *Coord. Chem. Rev*. **2017**, *349*, 139–155.

134. Wuttke, S.; Zimpel, A.; Bein, T.; Braig, S.; Stoiber, K.; Vollmar, A.; Müller, D.; Haastert-Talini, K.; Schaeske, J.; Stiesch, M.; et al. Validating Metal-Organic Framework Nanoparticles for Their Nanosafety in Diverse Biomedical Applications. *Adv. Healthc. Mater*. **2017**, *6*, 1600818.

135. Kumar, P.; Anand, B.; Tsang, Y.F.; Kim, K.H.; Khullar, S.; Wang, B. Regeneration, degradation, and toxicity effect of MOFs: Opportunities and challenges. *Environ. Res*. **2019**, *176*, 108488.

136. Sajid, M. Toxicity of nanoscale metal organic frameworks: A perspective. *Environ. Sci. Pollut. Res*. **2016**, *23*, 14805–14807.

137. Kumar, P.; Kaur N.; Tiwari P.; Gupta A.K.; Mobin S.M.; Gelatin-Coated Copper-Based Metal–Organic Framework for Controlled Insulin Delivery: Possibility toward Oral Delivery System. *ACS Materials Letters* **2023** *5* (4), 1100-1108.